## REFERENCES AND NOTES

1. D. L. Albritton, F. C. Fehsenfeld, A. F. Tuck, *Science* **250**, 75 (1990).
2. U. Platt, in *Air Monitoring by Spectroscopic Techniques, Chemical Analysis Series 127* (Wiley, New York, 1994), chap. 2.
3. R. D. Bojkov, *J. Clim. Appl. Meteorol.* **25**, 343 (1986).
4. E. Fonrobert, in *Chemie in Einzeldarstellungen* (Ferdinand Enke, Germany, 1916), vol. 9.
5. R. J. Strutt, *Proc. R. Soc. London A*, **94**, 260 (1918).
6. D. Chalonge and E. Vassy, *Rev. Opt.* **4**, 113 (1934).
7. A. Adel, *Astrophys. J.* **93**, 509 (1941).
8. M. V. Migeotte, *ibid.* **107**, 400 (1948).
9. A. Adel, *ibid.* **94**, 451 (1941).
10. M. V. Migeotte, *Phys. Rev.* **75**, 1108 (1949).
11. A. Adel, *ibid.*, p. 1766.
12. H. G. Reichle Jr. and H. A. Wallio, *J. Geophys. Res.* **91**, 9841 (1986); H. G. Reichle Jr. *et al.*, *ibid.* **95**, 9845 (1990).
13. M. Migeotte, L. Neven, J. Swenson, *Mem. Soc. R. Sci. Liege Spec. 1* (1956).
14. D. H. Ehhalt, U. Schmidt, R. Zander, P. Demoulin, C. P. Rinsland, *J. Geophys. Res.* **96**, 4985 (1991).
15. G. H. Mount, *ibid.* **97**, 2427 (1992).
16. D. Perner *et al.*, *Geophys. Res. Lett.* **3**, 466 (1976).
17. G. Hübler, D. Perner, U. Platt, A. Tönnissen, D. H. Ehhalt, *J. Geophys. Res.* **89**, 1309 (1984).
18. U. Platt, D. Perner, H. W. Pätz, *ibid.* **84**, 6329 (1979).
19. U. Platt and D. Perner, *Geophys. Res. Lett.* **7**, 89 (1980).
20. J. F. Noxon, R. B. Norton, E. Marovich, *ibid.*, p. 125.
21. H.-P. Dorn, U. Brandenberger, T. Brauers, M. Hausmann, D. H. Ehhalt, *ibid.* **23**, 2537 (1996).
22. H. K. Roscoe, D. J. Fish, R. L. Jones, *Appl. Opt.* **35**, 427 (1996).
23. J. P. Pommereau, in *Proceedings of the EUROTRAC Symposium 1990*, P. Borrell, Ed. (SPB Academic Publishing, The Hague, Netherlands, 1991), pp. 467–468.
24. A similar approach of wide bandwidth with an array detector was taken by J. M. C. Plane and C-F. Nien [*Rev. Sci. Instrum.* **63**, 1867 (1992)], who included the bands of $NO_3$.
25. E. Murray, in *Handbook of Air Pollution Analysis*, R. Perry and R. J. Young, Eds. (Chapman & Hall, London, 1977), chap. 8.
26. Unlike conventional lidar, the purpose of the time-of-flight information in this particular application of the Stanford lidar was to ensure that the chosen topographic target was observed and so the path length defined.
27. B. Galle, L. Klemedtsson, D. W. T. Griffith, *J. Geophys. Res.* **99**, 16575 (1994).
28. W. W. McMillan, L. L. Strow, W. L. Smith, H. E. Revercomb, H. L. Huang, *Geophys. Res. Lett.* **23**, 3199 (1996).
29. J. Pelon, P. Flamant, M. L. Chanin, G. Megie, in *Proceedings of the Quadrennial Ozone Symposium*, J. London, Ed. (IAMAP, Boulder, CO 1981), p. 130.
30. E. V. Browell, A. F. Carter, S. T. Shipley, in *Proceedings of the Quadrennial Ozone Symposium*, J. London, Ed. (IAMAP, Boulder, CO, (1981), pp. 99–107.
31. A. M. South *et al.*, abstract 416 of the Quadrennial Ozone Symposium book of abstracts (1996).
32. A. Volz-Thomas and B. A. Ridley, *Scientific Assessment of Ozone Depletion: 1994* (WMO Report 37, World Meteorological Organization, Geneva, Switzerland, 1995), chap. 5.
33. C. E. Canosa-Mas *et al.*, *J. Chem. Soc. Faraday Trans.* **92**, 2211 (1996).
34. W. R. Stockwell, J. B. Milford, D. Gao, Y-J. Yang, *Atmos. Environ.* **29A**, 1591 (1995).
35. A. C. Lewis, P. W. Seakins, A. M. Denha, K. D. Bartle, M. J. Pilling, *ibid.*, p. 1871.
36. S. A. Penkett *et al.*, *J. Geophys. Res.* **98**, 2865 (1993).
37. G. J. Wendel, D. H. Stedman, C. A. Cantrell, L. Danrauer, *Anal. Chem.* **55**, 937 (1983).
38. Two molecules of $NO_2$ are believed to be involved [C. A. Cantrell *et al.*, *J. Geophys. Res.* **98**, 2897 (1993)].
39. T. J. Kelly, C. W. Spicer, G. F. Ward, *Atmos. Environ.* **24A**, 2397 (1990).
40. H. I. Schiff, D. Pepper, B. A. Ridley, *J. Geophys. Res.* **84**, 7895 (1979).
41. F. C. Fehsenfeld *et al.*, *ibid.* **92**, 14710 (1987).
42. M. McFarland *et al.*, *ibid.* **91**, 5421 (1986).
43. M. J. Bollinger, R. E. Sievers, D. W. Fahey, F. C. Fehsenfeld, *Anal. Chem.* **55**, 1980 (1983).
44. D. W. Fahey, C. S. Eubank, G. Hubler, F. C. Fehsenfeld, *J. Atmos. Chem.* **3**, 435 (1985).
45. D. R. Crosley, *J. Geophys. Res.* **101**, 2049 (1996).
46. C. A. Cantrell and D. H. Stedman, *Geophys. Res. Lett.* **9**, 846 (1982).
47. D. R. Hastie, M. Weissenmayer, J. P. Burrows, G. W. Harris, *Anal. Chem.* **63**, 2048 (1991).
48. D. Mihelcic and A. Volz-Tomas, in *Proceedings of the EUROTRAC Symposium*, P. Borrell, P. M. Borrell, W. Seiler, Eds. (SPB Academic Publishing, The Hague, Netherlands, 1994), pp. 379–383.
49. A. Volz-Thomas *et al.*, in *Proceedings of the EUROTRAC Symposium*, P. M. Borrell, P. Borrell, T. Cvitas, K. Kelly, W. Seiler, Eds. (SPB Academic Publishing, The Hague, Netherlands, 1996), pp. 621–626.
50. H. E. Heitlinger *et al.*, in press.
51. D. Mihelcic, P. Muesgen, D. H Ehhalt, *J. Atmos. Chem.* **3**, 341 (1985).
52. D. Mihelcic, D. Klemp, P. Muesgen, H. W. Paetz, A. Volz-Thomas, *ibid.* **16**, 313 (1993).
53. T. M. Hard, R. J. O'Brien, C. Y. Chan, A. A. Merhrabzadeh, *Environ. Sci. Technol.* **18**, 768 (1984).
54. G. H. Mount and F. L. Eisele, *Science* **256**, 1187 (1992).
55. T. Brauers *et al.*, *Geophys. Res. Lett.* **23**, 2545 (1996).
56. M. K. Dubey, T. F. Hanisco, P. O. Wennberg, J. G. Anderson, *ibid.*, p. 3215.
57. F. L. Eisele *et al.*, *J. Geophys. Res.* **99**, 18605 (1994).
58. D. J. Tanner and F. L. Eisele, *ibid.* **100**, 2883 (1995).
59. C. A. Cantrell, R. E. Shetter, D. J. Tanner, F. L. Eisele, *Eos Trans.* **77**, 46 (1996).
60. T. Reiner, M. Hanke, F. Arnold, *J. Geophys. Res.* **102**, 1311 (1997).
61. A. A. Viggiano, *Mass Spectrom. Rev.* **12**, 115 (1993).
62. R. E. Shetter, A. H. McDaniel, C. A. Cantrell, S. Madronich, J. G. Calvert, *J. Geophys. Res.* **97**, 10349 (1992).
63. K. O. Lantz, R. E. Shetter, C. A. Cantrell, S. J. Flocke, J. G. Calvert, S. Madronich, *ibid.* **101**, 14613 (1996).
64. W. Junkermann, U. Platt, A. Volz, *J. Atmos. Chem.* **8**, 203 (1989).
65. A. Volz-Thomas *et al.*, *J. Geophys. Res.* **101**, 18613 (1996).
66. G. Baumbach and U. Vogt, *EUROTRAC Newsl.* **16**, 23 (1995).
67. J. M. Hoell *et al.*, *J. Geophys. Res.* **101**, 1641 (1996).
68. H. Worden, R. Beer, C. P. Rinsland, *ibid.* **102**, 1287 (1997).
69. R. L. Jones, personal communication.
70. S. Kawata, Y. Inouye, S. Minami, *SPIE* **1145**, 567 (1989).
71. J. Linkeman, F. Romero-Borja, H. O. Tittel, *ibid.* **1575**, 184 (1991).
72. J. E. Lovelock, R. J. Maggs, R. J. Wade, *Nature* **241**, 194 (1973).
73. W. Schrimpf, K. P. Muller, F. J. Johnen, K. Lienaerts, J. Rudolph, *J. Atmos. Chem.* **22**, 303 (1995).
74. E. Atlas, W. Pollock, J. Greenberg, L. Heidt, A. M. Thompson, *J. Geophys. Res.* **98**, 16933 (1993).


75. We thank R. L. Jones, D. J. Fish, R. A. Cox, P. E. Morris, D. A. Peel, and an anonymous referee for helpful discussions and comment.


# Cloud Microphysics and Climate


M. B. Baker



**Recent studies have shown that global radiative and hydrological fluxes are strongly linked to microphysical processes in clouds. The sensitivity of predictions of climate variations to assumptions about the microphysical processes has led to new approaches to atmospheric measurements and to heightened interest and progress in understanding the physical chemistry, radiative properties, and kinetics of small solid and liquid aqueous particles.**


Clouds cover almost two thirds of the global surface. They reflect incoming solar radiation, thus cooling the Earth-atmosphere system, and reduce outgoing infrared radiation, warming the system. Clouds also regulate the atmospheric hydrological cycle, transporting water away from Earth's surface, redistributing it through the atmosphere and back to the surface by means of precipitation. Latent heating and cooling associated with clouds modify atmospheric circulations, and thunderclouds produce lightning.

All of these phenomena have their origins in cloud microphysical processes, that is, processes involving ice and liquid-water particles whose dimensions range from under a micrometer to a few millimeters. Changes in cloud microphysical processes can modify the spatial extent, spatial distribution, and lifetimes of clouds, the water vapor distribution outside of clouds, and the fluxes of water and radiation through the atmosphere. This article focuses on the resulting changes in the distribution of atmospheric water and in the radiative fluxes at the top of the atmosphere (TOA). The discussion is centered on the following illustrative issues: possible modification of TOA radiative fluxes by anthropogenic aerosol particles in clouds, the impacts of ice particles on the TOA radiative fluxes, and the roles of cloud microphysical processes in regulating the atmospheric hydrological cycle.

The links between cloud microphysical parameters and the TOA radiative fluxes can be understood from a brief summary of Earth's radiation budget. The incoming TOA flux of solar radiation is about 340 $W/m^2$ on a global, annual average and is concentrated at short wavelengths ($\lambda \leq 4$ $\mu$m). About 30% of this energy is reflected


The author is in the Geophysics Program and Atmospheric Sciences Department, University of Washington, Seattle, WA 98195, USA.

by the system, partly by clouds, and the rest of the energy is absorbed, mainly at the surface. The shortwave flux absorbed by the system is balanced by the outgoing TOA long-wave flux, which peaks at $\lambda \approx 11$ μm. Part of this outgoing radiation is emitted by clouds. The shortwave reflectance, or albedo, of a cloud depends on the numbers and sizes of the water and ice particles in it, and the long-wave emissivity of a cloud depends on the total amount of condensed water. According to two-stream radiative transfer models, the albedo of a nonabsorbing homogeneous layer cloud over a nonreflecting surface is (*1*)

$$A_{\text{cloud}} \approx \frac{\tau_{sw}}{(1-g)^{-1}1 + \tau_{sw}} \quad (1)$$

where $g$ is a measure of the fraction of scattered light that propagates in the forward direction, and $\tau_{sw}$ is the optical depth of the cloud at solar wavelengths (the ratio of its geometric thickness $h$ to the mean free path of photons traversing it). To first approximation

$$\tau_{sw} \approx hN\, 2\pi r_{\text{eff}}^2 \quad (2)$$

where $N$ is the concentration of cloud particles, and $r_{\text{eff}}$ is a mean effective radius for scattering of shortwave radiation. Equation 1 is a reasonable approximation for thick boundary-layer clouds over mid-latitude oceans, where typical values are $r_{\text{eff}} \approx 10$ μm, $h \approx 250$ m, $N \approx 5 \times 10^7$ droplets m$^{-3}$, and $g \approx 0.8$, so that $\tau_{sw} \approx 6$ and $A_{\text{cloud}} \approx 0.55$. For these parameter values, the long-wave emissivity of the layer cloud is close to 1 at $\lambda \approx 11$ μm.

One measure of the impact of clouds on the absorbed shortwave radiation is the shortwave TOA cloud radiative forcing $CRF_{sw}$, defined as the absorbed shortwave radiation averaged over all regions of the sky minus that averaged over cloud-free regions. Because clouds are relatively efficient reflectors of solar radiation, $CRF_{sw}$ is negative. The corresponding impact of clouds on the TOA outgoing long-wave radiation is the long-wave cloud radiative forcing $CRF_{lw}$, defined as the outgoing long-wave radiation averaged over cloud-free regions of the sky minus that averaged over all regions. Because clouds in general emit at colder temperatures than do the parts of Earth's surface below them, $CRF_{lw}$ is positive and is maximum for high, cold clouds. The measured global mean net cloud effect on the radiative flux absorbed by the Earth-atmosphere system is $CRF_{net} = CRF_{sw} + CRF_{lw} \approx -20$ W/m$^2$ (*2*): The negative value means that, on average, clouds in the present atmosphere cool the system.

The net annual CRF measured by satellite varies greatly around the globe (Fig. 1) (*3*), corresponding to different types and spatial distributions of clouds in different regions: Marine stratiform clouds in the planetary boundary layer (where $CRF_{lw} \approx 0$) are responsible for most of the cooling, whereas deep convective cloud anvils and cirrus clouds at the top of the troposphere are responsible for much of the warming. The magnitudes of $CRF_{sw}$ and $CRF_{lw}$ depend on cloud extent, cloud vertical distribution, and cloud optical depths and emissivities. Modifications in these parameters result from changes in cloud particle concentrations, shapes, and sizes.

Water fluxes in the atmosphere are also determined in part by cloud microphysical properties. Precipitation is the sedimentation flux of those drops and ice particles whose terminal fall velocities are greater than the updraft velocity of the air; the flux depends strongly on the concentrations and types of the cloud particles.

Quantitative estimates of large-scale radiative and water fluxes in the atmosphere, and their responses to changing conditions, must rely on the predictions of general circulation models (GCMs). These models are sensitive to assumptions about microphysical parameters they cannot resolve (*4–8*). An early GCM study suggested, for example, that a decrease of less than 2 μm in the assumed mean radius of droplets in boundary-layer clouds would lead to a change in $CRF_{sw}$ that would approximately cancel the change in emitted long-wave flux due to an instantaneous global doubling of atmospheric $CO_2$ (*4*). The sensitivity of model predictions to variations in representations of cloud microphysical quantities provides strong motivation to improve our understanding of the microphysical processes and their impacts on climate.

## Anthropogenic Effects on CRF

Anthropogenic production of submicrometer particles (called aerosol particles) may increase the cloud droplet concentration $N$ in low clouds, increasing $\tau_{sw}$ (Eq. 2) and $A_{\text{cloud}}$ (Eq. 1) (*9*) and producing a change $\Delta CRF_{sw} < 0$. From Eq. 1 and a simple approximation for the transmission of shortwave radiation through the overlying atmosphere, it can be shown that an estimated change $\Delta CRF_{sw} \approx -1$ W/m$^2$ is produced by an increase $\Delta N/N \approx 30\%$ for low-level clouds in the Northern Hemisphere, all other factors remaining unchanged (*9–11*). In general, 100 cm$^{-3}$ $\leq N \leq$ 2000 cm$^{-3}$ in continental clouds, and 10 cm$^{-3}$ $\leq N \leq$ 100 cm$^{-3}$ over remote marine areas (*12*) (a difference that itself may be largely anthropogenic in origin). Therefore, for given $\Delta N$, the predicted change in albedo is largest over the oceans.

An increase in anthropogenic-aerosol concentrations might also give rise to $\Delta CRF_{sw} < 0$ if the increase produced in $N$ leads to a decrease in droplet radii and precipitation rate and an increase in cloud liquid-water content, cloud thicknesses, and cloud lifetimes (*13*). The result of the proposed two-stage process by which (i) increased aerosol concentrations modify cloud properties and (ii) the modifications in cloud properties result in increased cloud albedo (and $\Delta CRF_{sw} < 0$) is called the indirect radiative effect of aerosol particles. (Their direct radiative effect is modification of the optical properties of clear air.) Anthropogenic particles are most highly concentrated in the lower atmosphere (Fig. 2), so the indirect effect is expected to be most important in low-level marine clouds, which are those corresponding to the most negative CRF (the orange and red areas in Fig. 1).

The expectation that increased aerosol particle production will increase $N$ is based on the fact that cloud droplet formation at temperatures above 0°C begins with the condensation of vapor on partially wettable aerosol particles (largely sulfates, nitrates, sea salt in marine areas, and soluble organics). Not all of these become cloud droplets, however: At an environmental relative hu-

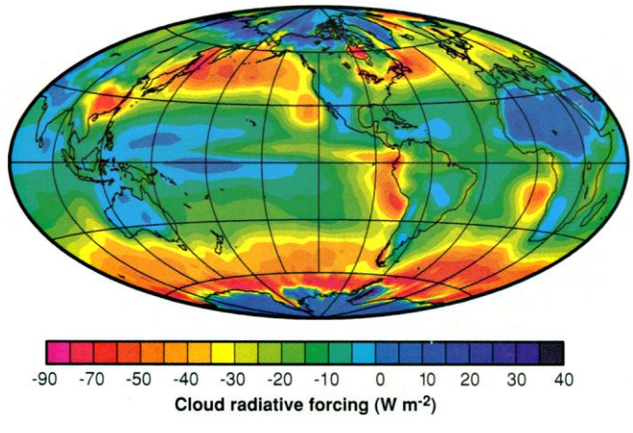


**Fig. 1.** Annual mean net CRF estimated from the Earth Radiation Budget Experiment (ERBE) scanning radiometer measurements from 1985 to 1986. Orange and red correspond to a strong cooling effect, whereas blue and green indicate warming. Values over snow-covered regions are probably unreliable. [Reproduced with permission from D. Hartmann]

midity RH ≈ 80%, or saturation ratio $S \equiv 0.01(\mathrm{RH}) \approx 0.8$, the soluble aerosol components are mostly dissolved, and the originally solid particles become solution droplets, called haze droplets, typically 0.01 to 0.1 μm in radius. A haze droplet of radius $r_d$ can remain in equilibrium as S increases so long as $S = S_{eq}(r_d)$ (*12*), where the equilibrium value $S_{eq}(r_d)$ depends on the surface energy of the liquid against the vapor $\sigma_{lv}$ (itself a function of the chemical composition of the droplet) and on the water activity $a_w$ (which decreases with increasing droplet solute concentration). Those droplets that grow by means of vapor deposition past the equilibrium range are said to activate, that is, they become cloud droplets; $S_{eq}(r_d) \rightarrow 1$ as $r_d$ increases, and the droplets continue to grow for any value $S \geq 1$. Thus, the concentration of cloud droplets at the cloud base N depends on the rate at which water vapor is supplied by cooling (a function of updraft velocity and the thermodynamic structure of the environment) and on the numbers, sizes, and chemical compositions of the aerosol particles.

Most modeling studies of the indirect radiative effect have concentrated on anthropogenic sulfate aerosols. Results of a GCM calculation (*5*) suggest that changes in sulfate aerosol distributions accompanying the Industrial Revolution have increased N by ≈0 to 20% over the Southern Hemisphere (SH) oceans and by ≈100% over the Northern Hemisphere (NH) continents. The associated indirect effect $\Delta\mathrm{CRF}_{sw} \approx -1$ W/m$^2$ (calculated with uncertainties of at least this magnitude) (*5, 7*) is consistent with that derived from the assumption that the mean difference (inferred from satellite measurements) between the NH and SH values of $r_{eff}$ [$\langle r_{eff}(\mathrm{SH}) - r_{eff}(\mathrm{NH})\rangle \approx 1$ μm] (*14*) is entirely a result of anthropogenic particle production.

The clearest observational evidence for an indirect aerosol effect is provided by ship tracks, which are trails (evident in satellite images) in ambient low-level clouds that result from the effluent from ships (*15*). Enhancement of liquid-water content in the ship tracks, possibly due to suppression of drizzle, and the reduction of $r_{eff}$ both contribute to the increase in reflectivity by increasing $\tau_{sw}$.

In general, however, it is difficult to isolate and quantify the aerosol indirect effect on the basis of measurements. One reason for this difficulty lies in measurement limitations. Cloud microphysical parameters ($r_{eff}$, N, and aerosol numbers and properties) are estimated from in situ (aircraft based) and remote (surface and satellite based) sensors; in general, the former are extremely limited in time and space but provide information with spatial resolution on the order of meters, whereas the spaceborne sensors can have near global coverage but resolutions typically on the order of kilometers. Aircraft instrumentation includes optical particle detectors and counterflow virtual impactors (CVIs) (*16*), which sample all particles over a minimum preset size, evaporate them, and measure the total evaporated water plus the number and types of residual aerosol particles. Satellite measurements of cloud parameters are actually inferences (called retrievals), made on the basis of numerical models, from the upwelling radiances at several different wavelengths in the visible and infrared. For low clouds, the measurement uncertainties in $r_{eff}$ are up to ±1 to 2 μm (*17*) for both satellite-based and in situ instruments. Thus, the mean NH-SH difference in $r_{eff}$ (*14*) is on the order of the random uncertainties in individual measurements.

Identifying anthropogenic influences on the measured relations between N and aerosol concentrations is complicated by variability in the thermodynamic properties of the air entering the cloud base, in the air motions, and in the amount of light-absorbing aerosol material in the cloudy air, which can cause variations in N and $A_{cloud}$ that can mask variations due to fluctuations in aerosol concentrations (*18*). In addition, the relations linking N to aerosol population parameters are nonlinear and variable (*5*), largely because aerosol chemistry, on which these relations depend, is complex (*19*). The traditional view, that aerosol composition is almost always dominated by sulfates, has been modified by recent observations (*20*) showing that up to 50% of the aerosol mass is composed of organic compounds, some of which are at least partially water soluble. Although the organic compounds have been identified previously in other contexts, the kinetic consequences of their presence in small droplets are as yet imperfectly understood. The diffusional growth and evaporation of a droplet of radius $r_d$ is driven by the difference $S - S_{eq}(r_d)$. The rate of growth or evaporation is controlled by the diffusion of heat and moisture between the droplet and the surrounding environment, and by impedance at the particle surface to the passage of water molecules across it (*12, 21*). Water-soluble organics are surface active; their effects on $S_{eq}$ through modification of $\sigma_{lv}$, $a_w$, and the surface impedance might alter activation behavior (*22*), the size distribution of the droplets, and cloud albedos.

The relations linking aerosol concentrations to N are further complicated by processes occurring after the aerosol particles leave their source. It is estimated that 80 to 90% of the atmospheric sulfate is formed on existing particles through oxidation of $SO_2$ in cloud droplets (*23*). Evaporation of cloud droplets can therefore leave a particle size distribution that is significantly different from the initial distribution (*24, 25*). The optical depth of aerosol particles (in clear air) and of subsequent clouds can be modified quite substantially by this cloud processing, an interesting feedback that may have important ramifications for global radiative balance. Calculations suggest that cloud processing may contribute $\Delta\mathrm{CRF}_{sw} \approx -1$ W/m$^2$ in the NH (*26*). The magnitude of the effect depends on the sizes and numbers of the unprocessed aerosol particles (*27*) and on precipitation rates; the rate of production of sulfate (aqueous-phase oxidation) in polluted clouds is roughly comparable to the average rate of loss over midlatitude oceans as a result of rainout. The potential importance of anthropogenic aerosol production to cloud albedos cannot be properly assessed without self-consistent treatment of the interdependent microphysical, chemical, and dynamic processes that characterize the aerosol-cloud system in the atmosphere.

## Ice-Particle Formation and Radiative Forcing

The relations between cloud droplet formation and radiative and hydrological fluxes in warm clouds are relatively simple, in principle, because cloud droplets are all similar in shape, and there is only one droplet formation process active in the atmosphere (although its quantitative details, as shown earlier, are not always predictable). In contrast, ice particles form and grow by a number of different mechanisms, have a wide range of shapes, and play a range of climatic roles. The importance to climate studies of small atmospheric ice particles is evident in the sensitivity of GCMs to different assumptions about these processes: Predicted CRF values change by 10 W/m$^2$ or more as a result of variation in the descriptions, all consistent with current understanding, of ice formation rates and growth of ice to the precipitation stage (*6*).

Mechanisms of ice particle formation and growth rates (and, therefore, the effects of ice particles on CRF and precipitation formation) are highly sensitive to temperature, humidity, and atmospheric composition. The two atmospheric regimes of interest are the mixed-phase region, in which supercooled water droplets and ice particles coexist, and the region of colder temperatures, at which clouds are fully glaciated.

*Ice formation in the mixed-phase region.* Supercooled water droplets and ice particles coexist in clouds over a range of tempera-

tures $0°C \geq T \geq T_{glac}$. The glaciation temperature $T_{glac}$ (below which all liquid particles have frozen) is extremely variable and can be above −10°C; for comparison, the homogeneous freezing temperature of pure water droplets in clouds is around −35°C. Liquid droplets can evaporate in the mixed-phase region, and ice particles can grow at their expense, because of the difference in their equilibrium vapor pressures. Latent heat associated with phase changes in this region is an important factor in modulating the vertical air motions that in turn transport the particles; thus, evolution of the cloud particles influences the extent and distribution of cloudiness, precipitation, and CRF. Variation of $T_{glac}$ from 0° to −40°C in a GCM (6) yielded $\Delta CRF_{lw} \approx 4$ W/m$^2$ and $\Delta CRF_{sw} \approx -8$ W/m$^2$, largely because of these dynamic consequences of the glaciation. These changes are not negligible with respect to mean measured values of $CRF_{sw}$ and $CRF_{lw}$; diminishing the uncertainty in $T_{glac}$ is thus a goal of importance for climate studies. This goal has not been achieved to date because of large uncertainties surrounding ice particle formation and growth.

In the mixed-phase region, the initial formation of ice is most often by heterogeneous nucleation from supercooled water on particles known as ice nuclei (IN), whose effectiveness depends on temperature and environmental humidity (*28, 29*) and on poorly understood characteristics of the particle surfaces (*30*). There is no satisfactory theory of heterogeneous ice nucleation, and no systematic, widespread system for collection of data on atmospheric IN activity. The concentrations of IN are low: Typical concentrations of pristine ice particles in clouds are ≈100 m$^{-3}$ at $T \approx -15°C$; thus, only about 1 aerosol particle in $10^8$ appears to function as an IN at this temperature. Until recently, relatively little was known about IN distributions in the atmosphere; however, as a result of several directed field campaigns and new instrumentation (*31*), a picture of the factors determining this distribution is beginning to emerge.

Measurements show that there are sources of IN at Earth's surface and that concentrations at a given location can vary substantially in time on seasonal and longer scales (*32, 33*), which may reflect variations in circulation patterns as well as those of IN source rates. Anthropogenic influences can both increase and decrease local IN distributions in the lower atmosphere (*12, 30*). The vertical profiles of active IN aloft can be complex (indicating multiple IN sources or circulation effects) (*34*). This finding contrasts with the assumption usually made in numerical models, namely, that the concentration of active IN depends only on temperature or relative humidity with respect to ice.

Biological materials—such as bacterial protein fragments, some as small as 0.01 μm in size, and even individual amino acids—can act as IN in supercooled drops at temperatures even above −5°C (*12, 30, 32*). This finding suggests that the structure of the water surrounding these particles is organized in a manner that decreases the energy barrier to nucleation, and it implies that there are interesting links between the biosphere and atmosphere that are of possible importance in changing climates. However, the existing field data are too sparse to determine the atmospheric roles of biogenic nuclei. At lower temperatures, clays and other water-insoluble particles have also been identified as IN.

The concentrations of small ice crystals at $T > -12°C$ are frequently many orders of magnitude higher, and much less dependent on temperature, than would be expected on the basis of heterogeneous ice nucleation alone. This long-standing puzzle in cloud physics has been partially resolved by systematic field studies in a range of cloud types (*35*); these studies show that most, but not all, of the observations of large concentrations of small ice particles at these high temperatures are consistent with laboratory observations of secondary ice production (that is, production by a mechanism that requires the prior existence of some ice) by means of fragmentation of freezing supercooled drops that collide with ice particles (*36*). Overlying cirrus clouds may also be an important source of secondary ice production in lower clouds, if ice particles sediment from the upper clouds without sublimating completely (*37*) (Fig. 2). The climatology of this natural ice-seeding mechanism is not well known, and in general, the secondary ice production mechanisms are not included in GCMs.

Atmospheric measurements thus provide insight into the atmospheric distribution of ice formation rates. However, in view of the sensitivity of atmospheric radiative and hydrologic fluxes to variations in these rates, the paucity of data and lack of a theory to explain them constitute important gaps in the present understanding of cloud microphysics.

*Ice formation in the upper troposphere.* In the upper troposphere, the mixing ratio of water vapor is too low to produce much ice, and the vertical motions in the clouds are gentle. Thus, the impact of ice formation and growth in these clouds (upper left corner of Fig. 2) on CRF is due primarily to the particle-radiation interactions themselves rather than their effects on precipitation or cloud dynamics. In situ measurements of ice particle properties are made by optical probes, replicators [coated slides (*38*) or films (*39*) that record the images of impacting crystals], and CVIs (*40, 41*), which have revealed that most of the crystals in mid-latitude cirrus clouds are smaller than 50 μm in their largest dimension (*40, 42*). Most of the IR absorption and much of the reflectivity in the visible is due to the small crystals. In tropical cirrus clouds (contributors to the dark-blue and green areas over the tropical Pacific Ocean in Fig. 1), the results of a numerical model (*8*) showed that small crystals ($r_{eff} < 20$ μm) contribute less than about 2% of the condensed water mass but backscatter about 4 W/m$^2$ of incoming solar radiation, enough to offset the global effect of

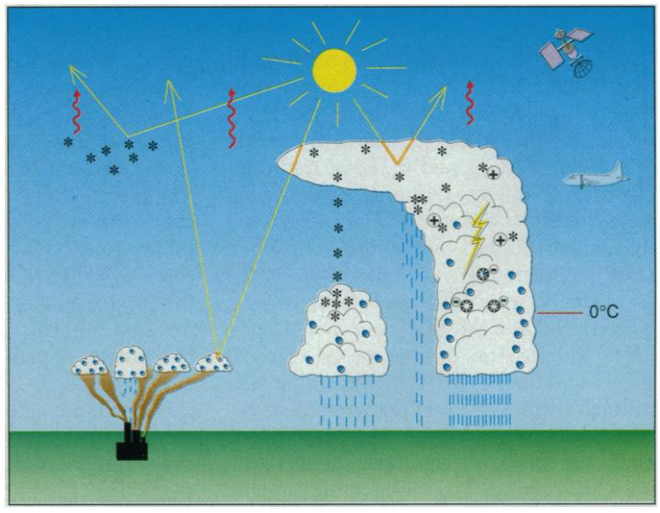


**Fig. 2.** Schematic representation of cloud microphysical processes discussed in this article. Clouds containing ice particles (*) and liquid drops (blue dots) contribute to long-wave (red wavy arrows) and solar (yellow arrows) radiative fluxes, shown at the top of the atmosphere. Anthropogenic aerosol particles (brown plumes) may modify the radiative properties of clouds. Precipitation (blue dashed lines) delivers water to Earth and redistributes water in the atmosphere. Soft hail particles (white snowflake in black circle) and ice crystals can become electrically charged during collisions, leading to lightning (jagged yellow symbol). [Figure created by K. Moore]

a doubling in the atmospheric concentration of $CO_2$. Therefore, prediction of the contribution to CRF by cirrus clouds requires computation of the rates of formation, growth, and shape evolution of the small ice particles as functions of the thermodynamic, dynamic, and chemical properties of the upper atmosphere. Because of the difficulty of in situ sampling in this region, and because these parameter regimes had not been well studied in the laboratory previously, most current thinking about these processes is based on developments made in the past few years.

Recent measurements in wave clouds (in which the particles form in situ and can be followed as they evolve) show the existence of liquid droplets that disappear as the ambient temperature falls below about $T \approx -35$°C (*43*). The droplets are replaced by larger ice crystals, after which the relative humidity stays constant at the ice saturation value.

These observations suggest that the dominant mechanism of ice formation at $T \leq -35$°C is the homogeneous nucleation of ice by the freezing of small liquid-solution droplets; this suggestion is supported by the finding that the concentrations of IN in background air are often quite low in the upper troposphere (*34*). Calculations of the rates of formation of ice particles in the upper troposphere are therefore usually based on the classical homogeneous nucleation theory, according to which the rate of formation of ice embryos is

$$J(T) \propto \exp(-\Delta G_{crit}/kT) \quad (3)$$

where $\Delta G_{crit} = \Delta G_{act} + \Delta G_{surf}$, $\Delta G_{act}$ is the energy required for a molecule to escape from the liquid and become incorporated in the ice lattice, and $\Delta G_{surf}$ is the minimum work required to form an ice embryo. These energies depend on $\sigma_{il}$ (the effective interfacial energy of ice against the liquid) and the water activity in the liquid solution. For pure water, the freezing rates predicted by this theory, using commonly accepted parameter values, have differed by orders of magnitude from those measured in the laboratory, and $\Delta G_{act}$ and $\sigma_{il}$ have traditionally been adjusted to diminish the differences (*12, 44*). However, classical theory does fit the laboratory observations well when these parameters are obtained from a new equation of state of water (*45*) based on current theories of the supercooled state (*46*). Despite the limitations of classical theory to describe the fluctuations that lead to nucleation, the excellent agreement between experiments and the predictions based on the new equation of state represents an interesting example of the growing relevance to atmospheric science of detailed studies on water substance.

This treatment has not been extended to the case of cirrus clouds, in which the droplets are probably concentrated solutions of sulfuric acid, ammonium sulfate, and possibly other nitrogen compounds formed on deliquescent aerosols. These particles may be formed aloft by gas-to-particle conversion in clear air (*47*); in addition, some originate from volcanoes, and some arise from anthropogenic sources [such as high flying aircraft (*48*)], suggesting the possibility of at least a localized indirect aerosol effect at high altitudes. Soot has been mentioned (*48, 49*) as a possibly important ice-nucleating component of the jet contrails, suggesting that, as in the lower atmosphere, carbonaceous components of aerosol particles cannot be neglected in estimating anthropogenic effects on CRF. However, the importance of this source is unclear, in part because of uncertainties regarding the physical chemistry of the nucleation pathways (*48*).

As solution droplets ascend from below, their properties depend on the relative humidity they encounter. The equilibrium vapor pressure over a solution droplet decreases with increasing solute concentration; thus, at low humidities (which are associated in the atmosphere with low air temperatures), only highly concentrated, small droplets are still liquid. Prediction of homogeneous nucleation rates for these concentrated solution droplets through application of classical nucleation theory requires data on the activity coefficients $a_w$ at low temperatures and the values of $\Delta G_{act}$ and $\sigma_{il}$ in highly concentrated aqueous solutions, now a subject of active research in several laboratories (*50*).

The rates of formation and growth of ice particles in mid-latitude cirrus clouds appear to be primarily determined by the availability of water vapor rather than by the concentration of unfrozen haze droplets. These haze droplets may be responsible for the so-called subvisible cirrus, optically thin clouds at cirrus altitudes (*40, 51*). An alternative explanation for subvisible cirrus is that they consist of small ice particles that sublimate slowly because of high surface impedance, possibly caused by foreign (nonwater) molecules near the particle surface (*52, 53*). The sublimation rates of small atmospheric ice particles depend (as in the droplet case) on the local humidity and on diffusion rates in the environment, and they also depend on the surface impedance to vapor transport. The latter term is important when the departure from equilibrium is small, the particles are small, and the ambient pressure is low—conditions that are present in cirrus clouds (*53*).

The radiative properties of ice clouds depend on crystal shapes as well as their concentrations and sizes. The faceted shapes of growing ice crystals are responsible for halos, sundogs, and other optical phenomena characteristic of cirrus clouds, most of which are not described by the radiative-transfer models that are used to predict the radiative properties of clouds and to interpret remotely sensed radiances. The two issues of importance are (i) computation of the radiative properties of ice crystals of realistic shapes and (ii) prediction of those shapes as functions of environmental conditions. Current uncertainties about the shapes of ice particle in cirrus clouds can produce errors in retrieved optical depths at visible wavelengths of up to a factor of 3 and in albedo retrievals of about 10 to 15% (*54*). Sophisticated techniques have been applied to the problem of computing light-scattering phase functions for crystals (*55*); laboratory measurements on growing and sublimating crystals are needed to confirm their results.

Ice particle shapes in cirrus clouds range from bullets, compact and hollow capped and uncapped columns, dendritic plates and bullet rosettes, to trigonal and nearly spherical particles; these last shapes are presumably due to evaporation under the conditions in the upper troposphere. The observed shapes show the complex dependence of the surface properties on temperature and humidity. At present there is no theoretical explanation for this dependence, which has long been known at higher temperatures (*56*), and all three-dimensional models of ice crystal growth include empirical parameterizations of the habit variations (*57*). It is not known whether impurities in the atmospheric environment have measurable effects on the evolution of crystal shape.

The dependence of crystal shapes and sizes on environmental conditions and growth history has important consequences for cirrus CRF. Ice crystals found high in the troposphere tend to be smaller than those at higher temperatures, and thus tend to backscatter more efficiently [larger $(1 - g)$ in Eq. 1], which increases cloud albedo. On the other hand, because the available water vapor decreases with increasing altitude, and because large particles sediment while growing, the ice content generally decreases with cloud altitude, which decreases $\tau_{sw}$ and cloud albedo, other things being equal. These opposing tendencies are relevant to an issue of current debate, namely, the thermostat hypothesis (*58*), which stems from the observation that for tropical cirrus clouds, variations in $CRF_{sw}$ and $CRF_{lw}$ are highly correlated, so that the response of these clouds to a perturbation in sea surface temperature might be $\Delta CRF_{net} = \Delta(CRF_{sw} + CRF_{lw}) \approx 0$. The high correlation of $\Delta CRF_{lw}$ and $\Delta CRF_{sw}$ might arise

(i) if cloud altitude is more or less invariant but both $\Delta CRF_{lw}$ and $\Delta CRF_{sw}$ are monotonic functions of cloud thickness, or (ii) if increased cloud thickness (and hence higher cloud emissivity and more positive $\Delta CRF_{lw}$) is always associated with higher clouds (lower cloud-top temperatures) and therefore with smaller particles (higher $A_{cloud}$) and more negative $\Delta CRF_{sw}$. Recent in situ observations (39) of tropical cirrus clouds suggest that the high albedos observed are mainly the result of increased ice-water content and increased cloud thicknesses over the Pacific "warm pool," a result that favors the first explanation.

## Cloud Microphysics and the Hydrological Cycle

The most obvious impact of clouds on the hydrological cycle is that of precipitation. In removing water from the atmosphere, precipitation modifies cloudiness and cloud structure. Moreover, the latent heating associated with precipitation is a driving force for atmospheric circulations (59). Precipitation and detrainment of cloud air to the environment also alter the distribution of water vapor in, and hence the radiative properties of, the air around them, an effect not explicitly accounted for in our definition of CRF.

Predicted values of CRF are highly sensitive to assumed changes in precipitation rates and distributions; variation of the rate of production of precipitation within the ranges of the microphysical parameterizations currently in use changes mid-level cloudiness in several GCM studies enough to produce variations in the magnitudes of $\Delta CRF_{lw}$ and $\Delta CRF_{sw}$ comparable with the global mean measured values of the CRF components.

Although most of the precipitation that forms in deep convective clouds falls back to Earth through the cloud base, some is detrained through stratiform anvils and cirrus clouds into unsaturated air. Precipitation also falls from upper level clouds and sublimates (Fig. 2). It has been suggested (60–62) that detrainment of cloud air (primarily, but not exclusively near the tropopause) and sublimation of the ice particles falling in unsaturated air constitute an important moisture source for the environment. The idea that ice crystal lofting is the dominant source of water vapor in the upper troposphere is supported by isotope analysis of crystals and estimates of the ice/vapor ratio at the cloud top (63). According to this suggestion, the pressure-dependent source of water vapor in the clear air outside of a cloud system depends on (i) the removal rate of precipitation before detrainment, (ii) the rate of evaporation (sublimation) of the condensate in descending parcels, and (iii) the fraction of the area over which water evaporates into clear air (64). All of these factors are determined by cloud microphysical processes. Although initial calculations (61) suggest that the hydrometeor sublimation hypothesis is consistent with measured profiles of mean relative humidity in the Hadley cell region, the calculated net moistening is extremely sensitive to ice particle formation rates, sublimation and vapor growth rates, terminal fall velocities [which range from $V_{snow} \approx 0.1$ m/s to $V_{hail} \approx 10$ to 50 m/s (65)], and the details of collisional processes. For example, because of the difference in terminal fall velocities, the mass loss rate from an evaporating raindrop 2 mm in diameter at $T = 0$°C is less than one third of that from a soft hail particle of the same diameter under the same conditions.

Our ability to quantify these effects of cloud microphysics on the hydrological cycle is limited because water fluxes in the atmosphere are not directly measurable and measurements of precipitation at the ground are inadequate for the purpose (66). Measurements of precipitation rates at ground-based stations (on areal scales of $\approx 10^{-8}$ to $10^{-6}$ km$^2$) are necessarily quite limited. Areal precipitation rates (both at the ground and aloft) have been deduced from radiative probes on satellites on areal scales of $\approx 100$ km$^2$ and from precipitation radar on the ground or aircraft, used to deduce areal rates on scales of 2 to 4 km$^2$. There are several problems inherent in these approaches (67), and comparison of rainfall rates estimated from a satellite with those measured at the surface often differ by factors of 2 to 3, especially over land. One problem is the obvious mismatch in measurement scales and sampling characteristics of the different sensors. The most serious weakness of the retrievals is that the radiances are not uniquely related to the physical parameters of interest; radiative transfer models and cloud models are necessary to convert the measured radiances to in-cloud precipitation fluxes, and more modeling is required to estimate precipitation falling in clear air and to the ground. An attempt to improve remote sensing of rainfall climatology will be the focus of a 3-year satellite study [Tropical Rainfall Measuring Mission (TRMM)] to begin in 1997 (68).

New measurement techniques may aid considerably in quantifying the distributions of water flux in clear air and their sensitivity to microphysical variations. One promising technique is the use of remotely piloted aircraft (69). It may also be possible to infer in-cloud water fluxes from observations of lightning flash rates, because of the role water fluxes play in lightning production. The high electric fields in thunderstorms arise largely from gravitational separation of heavy, negatively charged graupel particles and light, positively charged ice crystals (Fig. 2). The particles somehow become electrically charged (70) when they collide and then rebound in the mixed-phase region (71). Thus, lightning production depends on those factors (such as water flux into the mixed-phase region) that determine the sizes and numbers of large graupel particles and small ice crystals. Lightning frequency may provide information on the water fluxes and on the parameters at the surface that determine them (72), under conditions that have not been thoroughly explored (73). A "Lightning Imaging Sensor" is to be launched on a satellite as part of the TRMM mission. Part of its mission is to investigate the use of remote sensing of lightning distributions to supplement data on these climate parameters from other sources (74).

## Summary and Conclusions

At present, although the main feedback in climate models is that due to clear-sky water vapor, differences from model to model in the representation of microphysical processes are a major reason for differences in model predictions of climate sensitivity to external forcing (75). Constraints on these representations will require improved understanding of the microphysical processes both on the scale of individual particles and on the atmospheric scale. The physics and chemistry of small aqueous particles constitutes an important part of the study of climate; the laboratory and theoretical studies guide and are guided by atmospheric measurements that have led to significant changes in our understanding of the microphysical behavior.

The small-scale physical and chemical processes linking anthropogenic aerosol particles to droplet populations in the lower atmosphere and to ice-crystal populations in the upper atmosphere must be better understood in order to quantify the effects of anthropogenic aerosol particles on the albedos and extent of clouds. Similarly, detailed study of the physical chemistry and radiative properties of small atmospheric ice particles is necessary in order to interpret in situ measurements of the quantities determining the albedos, emissivities, cloud-top temperatures, and extent of cirrus clouds.

On the other hand, the major gaps in our understanding of the radiative roles of mixed-phase clouds result from a lack of climatological data on ice and precipitation formation in the middle troposphere.

New approaches to the measurement of atmospheric water fluxes inside, under, and in the vicinity of clouds will be required in order to determine the role of each of the microphysical processes discussed here in the global hydrological cycle.

## REFERENCES AND NOTES


1. J. Coakley and P. Chylek, *J. Atmos. Sci.* **32**, 409 (1975).
2. D. L. Hartmann, in *Aerosol-Cloud-Climate Interactions*, P. V. Hobbs, Ed. (Int. Geophys. Ser. 54, Academic Press, San Diego, (CA, 1993), pp. 151–173.
3. E. F. Harrison *et al.*, *J. Geophys. Res.* **95**, 18687 (1990); V. Ramanathan *et al.*, *Science* **243**, 57 (1989). This plot was first shown in S. A. Klein and D. L. Hartmann, *J. Clim.* **6**, 1587 (1993).
4. A. Slingo, *Nature* **343**, 49 (1990).
5. O. Boucher and U. Lohmann, *Tellus B* **47**, 281 (1995).
6. L. Fowler, D. Randall, S. Rutledge, *J. Clim.* **9**, 489 (1996).
7. A. Jones, D. Roberts, A. Slingo, *Nature* **370**, 450 (1994).
8. C. Zender and J. Kiehl, *J. Geophys. Res.* **99**, 25869 (1994).
9. S. Twomey, *Atmospheric Aerosols* (Elsevier, New York, 1977); *Atmos. Environ. A* **25**, 2435 (1991).
10. R. Charlson *et al.*, *Science* **255**, 423 (1992).
11. S. Schwartz, in *Clouds, Chemistry and Climate*, P. Crutzen and V. Ramanathan, Eds. (NATO ASI Ser. 1, Springer-Verlag, Berlin, 1996), vol. 35, pp. 191–236; P. V. Hobbs, in *Aerosol-Cloud-Climate Interactions*, P. V. Hobbs, Ed. (Int. Geophys. Ser. 54, Academic Press, San Diego, CA, 1993), pp. 35–69.
12. H. Pruppacher and J. Klett, *Microphysics of Clouds and Precipitation* (Reidel, Boston, 1978).
13. B. A. Albrecht, *Science* **245**, 1227 (1989); A. S. Ackerman, O. B. Toon, P. V. Hobbs, *ibid.* **262**, 226 (1993); R. Pincus and M. Baker, *Nature* **372**, 250 (1994).
14. Q. Han, W. Rossow, A. Lacis, *J. Clim.* **7**, 465 (1994).
15. J. A. Coakley Jr., R. L. Bernstein, P. A. Durkee, *Science* **237**, 1020 (1987); M. D. King, L. F. Radke, P. V. Hobbs, *J. Geophys. Res.* **98**, 2729 (1993).
16. J. A. Ogren, J. Heintzenberg, R. J. Charlson, *Geophys. Res. Lett.* **12**, 121 (1985).
17. J. Brenguier, D. Baumgardner, B. Baker, *J. Atmos. Oceanic Technol.* **11**, 1409 (1994); S. Platnick and F. Valero, *J. Atmos. Sci.* **52**, 2985 (1995).
18. Special issue on the Atlantic Stratocumulus Transition Experiment, *J. Atmos. Sci.* **52** (no. 16) (1995).
19. T. Anderson, G. Wolfe, S. G. Warren, in *Encyclopedia of Earth System Science* (Academic Press, New York, 1992), vol. 1, pp. 363–376.
20. W. H. White, in *Acidic Deposition State Science Rep. 24, no. 4* (National Academy of Precipitation Assessment Program, Washington, DC, 1990), pp. 90–94; T. Novakov and J. Penner, *Nature* **365**, 823 (1993).
21. D. E. Hagen *et al.*, *J. Atmos. Sci.* **46**, 803 (1989); P. Wagner, in *Topics in Current Physics*, W. H. Marlow, Ed. (Springer-Verlag, New York, 1982), pp. 129–178.
22. P. Saxena, L. Hildemann, P. McMurry, J. Seinfeld, *J. Geophys. Res.* **100**, 18755 (1995); M. Shulman, M. Jacobson, R. Charlson, R. Synovec, T. Young, *Geophys. Res. Lett.* **23**, 277 (1996).
23. J. Lelieveld, in *C,N,P and S Biogeochemical Cycles*, R. Wollast, Ed. (NATO ASI Ser. 1, Springer-Verlag, Berlin, 1992), pp. 305–332; D. Hegg, *J. Geophys. Res.* **90**, 3773 (1985).
24. D. Hegg, *Geophys. Res. Lett.* **17**, 2165 (1990).
25. W. Hoppel, J. Fitzgerald, C. Fink, R. Larson, E. Mack, *J. Geophys. Res.* **95**, 3659 (1990).
26. J. Lelieveld and J. Heintzenberg, *Science* **258**, 117 (1992).
27. D. Hegg, R. Majeed, P. Yuen, M. Baker, T. Larson, *Geophys. Res. Lett.* **23**, 2613 (1996).
28. N. Fletcher, *The Physics of Rainclouds* (Cambridge Univ. Press, Cambridge, 1962).
29. P. Meyers, P. DeMott, W. Cotton, *J. Appl. Meteorol.* **31**, 708 (1992).
30. G. Vali, *J. Rech. Atmos.* **19**, 105 (1985); R. Schnell and G. Vali, *J. Atmos. Sci.* **33**, 1554 (1976); W. Szyrmer and I. Zawadski, *Bull. Am. Meteorol. Soc.* **78**, 209 (1997).
31. D. Rogers, *Atmos. Res.* **29**, 209 (1993).
32. E. K. Bigg, *ibid.* **25**, 397 (1990).
33. ———, *Tellus B* **48**, 223 (1996).
34. R. Rasmussen, W. A. Cooper, P. DeMott, D. Rogers, in *Proc. AMS Conf. on Cloud Physics*, Dallas (American Meteorological Society, Boston, 1995), pp. 134–138.
35. P. V. Hobbs and A. Rangno, *J. Atmos. Sci.* **42**, 2523 (1985); A. Rangno and P. V. Hobbs, *Q. J. R. Meteorol. Soc.* **117**, 207 (1991); K. Bower *et al.*, *ibid.* **122**, 1815 (1996); A. Blyth and J. Latham, *ibid.* **119**, 91 (1993).
36. J. Hallett and S. Mossop, *Nature* **249**, 26 (1974); R. Chisnell and J. Latham, *Q. J. R. Meteorol. Soc.* **102**, 133 (1976).
37. W. Hall and H. Pruppacher, *J. Atmos. Sci.* **33**, 1995 (1976); R. Braham and P. Spyers-Duran, *J. Appl. Meteorol.* **6**, 1053 (1967).
38. J. Hallett, *U.S. Air Force Geophys. Lab. Contract AFGL-TR-76-0149* (1976).
39. A. Heymsfield and L. McFarquhar, *J. Atmos. Sci.* **53**, 2424 (1996).
40. J. Strom and J. Heintzenberg, *ibid.* **51**, 2368 (1994).
41. K. B. Noone, K. J. Noone, J. Heintzenberg, J. Strom, J. Ogren, *J. Atmos. Oceanic Technol.* **10**, 294 (1993).
42. W. Arnott, Y. Dong, J. Hallett, *J. Geophys. Res.* **99**, 1371 (1994).
43. A. Heymsfield and L. Miloshevich, *J. Atmos. Sci.* **52**, 4302 (1995).
44. P. DeMott and D. Rogers, *ibid.* **47**, 1056 (1990).
45. C. Jeffery and P. Austin, *J. Geophys. Res.*, in press.
46. P. Poole, F. Sciortino, T. Grande, H. Stanley, C. Angell, *Phys. Rev. Lett.* **73**, 1632 (1994).
47. K. Perry and P. V. Hobbs, *J. Geophys. Res.* **99**, 22803 (1994).
48. B. Karcher, Th. Peter, U. Biermann, U. Schumann, *J. Atmos. Sci.* **53**, 3066 (1996).
49. E. J. Jensen and O. Toon, *Geophys. Res. Lett.* **24**, 249 (1997); P. DeMott, *J. Appl. Meteorol.* **29**, 1072 (1990).
50. B. Luo, T. Peter, P. Crutzen, *Geophys. Res. Lett.* **21**, 1447 (1994); R. MacKenzie, M. Kulmala, A. Laaksonen, T. Vesala, *J. Geophys. Res.* **100**, 11275 (1995); D. Anderson and E. Betterton, in *Proc. AGU Conf.*, San Francisco (American Geophysical Union, Washington, DC, 1996), p. F95.
51. K. Sassen and B. Cho, *J. Appl. Meteorol.* **31**, 1275 (1992).
52. T. Deshler, Th. Peter, R. Müller, P. Crutzen, *Geophys. Res. Lett.* **21**, 1327 (1994).
53. J. Nelson and M. B. Baker, *J. Geophys. Res.* **101**, 7033 (1996); R. MacKenzie and P. Haynes, *J. Geophys. Res.* **97**, 8057 (1992); Th. Peter and M. B. Baker, in *Clouds, Chemistry and Climate*, P. Crutzen and V. Ramanathan, Eds. (NATO ASI Ser. 1, Springer-Verlag, Berlin, 1996), vol. 35, pp. 57–82.
54. A. Vogelmann and T. Ackerman, *J. Atmos. Sci.* **52**, 4285 (1995).
55. K.-N. Liou and N. Rao, *ibid.* **53**, 3046 (1996).
56. U. Nakaya, M. Hanajima, J. Mugurama, *J. Fac. Sci. Hokkaido Univ. Ser. 2* **5** (no. 3), 88 (1958); T. Kobayashi, *J. Meteorol. Soc. Jpn.* **43**, 359 (1965); D. Lamb and W. D. Scott, *J. Cryst. Growth* **12**, 21 (1972).
57. J. P. Chen and D. Lamb, *J. Atmos. Sci.* **51**, 1206 (1994).
58. V. Ramanathan and W. Collins, *Nature* **361**, 410 (1993).
59. S. Rutledge and R. Houze, *J. Atmos. Sci.* **44**, 2640 (1987).
60. A. Betts, *Bull. Am. Meteorol. Soc.* **71**, 1465 (1990).
61. D.-Z. Sun and R. Lindzen, *J. Atmos. Sci.* **50**, 1643 (1993).
62. K. Emanuel and R. Pierrehumbert, in *Clouds, Chemistry and Climate*, P. Crutzen and V. Ramanathan, Eds. (NATO ASI Ser. 1, Springer-Verlag, Berlin, 1996) vol. 35, pp. 17–28.
63. R. Smith, *J. Atmos. Sci.* **49**, 2041 (1992).
64. N. Renno, K. Emanuel, P. Stone, *J. Geophys. Res.* **99**, 14429 (1994).
65. R. Houze, *Cloud Dynamics*, R. Dmowska and J. Holton, Eds. (Int. Geophys. Ser. 53, Academic Press, San Diego, CA, 1993), chap. 3.
66. G. J. Huffman *et al.*, *Bull. Am. Meteorol. Soc.* **78**, 5 (1997).
67. C. Kummerow and L. Giglio, *J. Appl. Meteorol.* **33**, 19 (1994); R. Fulton and G. Heymsfield, *ibid.* **30**, 98 (1991).
68. J. Simpson, R. Adler, G. North, *Bull. Am. Meteorol. Soc.* **69**, 278 (1988).
69. K. Emanuel and R. Smith, in *AGU Chapman Conf. on Water Vapor in the Climate System*, Jekyll Isle, GA (American Geophysical Union, Washington, DC, 1994), p. 12.
70. J. Rydock and E. Williams, *Q. J. R. Meteorol. Soc.* **117**, 409 (1991); M. B. Baker and J. G. Dash, *J. Geophys. Res.* **99**, 10621 (1994).
71. S. Reynolds, M. Brook, M. Gourley, *J. Meteorol.* **14**, 426 (1957); T. Takahashi, *J. Atmos. Sci.* **35**, 1536 (1978); E. R. Jayaratne, C. Saunders, J. Hallett, *Q. J. R. Meteorol. Soc.* **109**, 609 (1983); B. Baker, M. Baker, E. R. Jayaratne, J. Latham, C. Saunders, *ibid.* **113**, 1193 (1987); E. Avila and G. Caranti, *J. Geophys. Res.* **99**, 10611 (1994).
72. E. R. Williams, *Science* **256**, 1184 (1992).
73. S. Sheridan, J. Griffiths, R. Orville, in *Proc. AGU Fall Meeting*, San Francisco (American Geophysical Union, Washington, DC, 1996), p. F90.
74. H. Christian *et al.*, in *Proc. 10th Int. Conf. on Atmospheric Electricity* (International Commission of Atmospheric Electricity, and Society of Atmospheric Electricity of Japan, Osaka, 1996), pp. 368–371.
75. R. Cess *et al.*, *J. Geophys. Res.* **101**, 12791 (1996).


76. Partial support for this work came from NSF grant ATM-9417745. I am very grateful for helpful suggestions and comments by a number of colleagues at the University of Washington and elsewhere.